CHAPTER IV

IMPORTANCE OF THE SOLID STATE OF 17β-ESTRADIOL ON ITS RELEASE CHARACTERISTIC FROM IMPLANT USING EUDRAGIT® RS AS A RELEASE CONTROLLING AGENT

4.1 Introduction

Over the last two decades, matrix system containing a poorly water-soluble drug and using an inert polymer as the matrix excipient has been widely investigated. Many researchers have indicated that it is possible to obtain a zero-order release kinetic from this controlling system (Chandrasekaran and Paul, 1982; Ford et al., 1987; El-Arini and Leuenberger, 1995; Kim, 2000b; Costa and Lobo, 2001; Siepmann and Peppas, 2001). Studies conducted by Ford et al. (Ford, Rubinstein, and Hogan, 1985a; 1985b; 1985c; Ford et al., 1987) reported that dissolution profiles of two insoluble drugs, indomethacin and diazepam, from hydroxypropylmethylcellulose (HPMC) matrices exhibited near zero-order release kinetics whereas dissolution profiles of soluble drugs, including promethazine hydrochloride, aminophylline, tetracycline hydrochloride and propranolol hydrochloride, from HPMC matrices exhibited square root of time kinetics. These studies corresponded to the one conducted by El-Arini and Leuenberger (1995) which indicated the zero-order release kinetic of caffeine representing a poorly water-soluble drug from polyvinylpyrrolidone (PVP) matrix and the square root of time kinetic of potassium chloride representing a water-soluble drug from the same polymeric matrix. Chandrasekaran and Paul (1982) indicated that the mass released had a square-root dependency with time in which dispersed matrix was totally controlled by diffusion process. On the contrary, the mass released varied directly with time or the release rate of a dispersed drug would become time independent in which drug dissolution offered the limiting resistance to mass transport. From previous chapter, the release kinetics of 17β-estradiol (E_2) and norethindrone (NET) from implants using Eudragit® RS (ERS) as a release controlling agent exhibited zero-order release kinetics. The obtained release kinetics did not result from the Geomatrix® design. Kim (2000b) indicated that geometry was not an important factor for a drug dissolution controlled release system. Furthermore, the porosity and the tortuosity did not play the leading role in controlling E_2 and NET released. In case of poorly water-soluble drug, dissolved drug and non-dissolved drug coexist within the polymer matrix. Siepmann and Peppas (2001) indicated that non-dissolved drug was not available for diffusion. Non-dissolved drug remaining within the polymer matrix resulted in drug concentration gradient unchanged and the absolute amount of drug released within a certain time period remained constant. This non-dissolved drug effect overcompensated the previously described porosity and geometry effect.

For polymer matrix containing poorly water-soluble drug, drug solubility under a given condition plays the leading role in controlling drug release. In the same way, the inherent solubility of E_2 under a given condition is a major factor affecting

release profile and release kinetics of E_2 implant using ERS as a release controlling agent. If the solubility of E_2 in the polymer matrix under a given condition changes, release profile and release kinetics of E_2 should be altered. In polymer matrix containing drug at concentration lower than its solubility in that polymer, drug exists in a dissolved state. On the contrary, drug exists in a crystalline state when its concentration in the polymer matrix is much higher than its solubility in that polymer. Patterson et al. (2006) indicated that an amorphous drug existed where drug was dispersed in the polymer on a molecular level. The solubility of a compound in the amorphous form is higher than that in the more stable crystalline form because the Gibbs free energy is higher (Martin, 1993). The dissolution rate of an amorphous compound is improved relative to a crystalline form (Patterson et al., 2006). Thus, release profile and release kinetics of amorphous E_2 should be different from those of a crystalline E_2.

The aims of this study were

(i) to determine the influence of solid state of E_2 on the E_2 release characteristic.

(ii) and to investigate the effect of weight percent of E_2 in ERS solid dispersions on the solid state of E_2.

4.2 Materials and Methods

4.2.1 Materials

17β-estradiol (E_2) and Benzalkonium chloride (BAC) were purchased from Fluka Chemica, Germany. Eudragit® RS PO (Röhm Pharma GmbH, Germany) was donated by JJ Degussa, Thailand. Absolute ethanol and dichloromethane were of a reagent grade purchased from Merck, Germany. Acetonitril was of a HPLC grade purchased from Fisher Scientific (UK). Sodium hydroxide and potassium dihydrogen phosphate were obtained from Mallinckrodt (Mexico) and Asia Pacific Specialty Chemicals Limited (Australia), respectively.

4.2.2 Preparation and Determination of E_2 Content in Solid Dispersions

Solid dispersions containing 10, 20 and 30 % w/w E_2 in ERS were prepared and E_2 content in each sample was determined as described in previous study. Solid dispersions containing 1 and 2 % w/w E_2 in ERS were prepared with the same procedure as those containing E_2 at concentration range of 10-30 % w/w, except when a mixture of absolute ethanol: dichloromethane (1:1; v:v) was used in the process of dissolving E_2 and ERS at mass ratios of 1/99 and 2/98.

4.2.3 Preparation of Implants

Implants containing 1 or 2 % w/w E_2 in ERS solid dispersions were produced by the same method as that of implants containing 10, 20 and 30 % w/w E_2 in ERS solid dispersions as described in previous chapter.

4.2.4 Drug Release Study

Release studies of implants containing 1 and 2 % w/w E_2 in ERS solid dispersion were conducted, in triplicate, in the same way as that of implants containing 10, 20 and 30 % w/w E_2 in ERS solid dispersion as described in previous study. Release medium of implants containing 1 and 2 % w/w E_2 in ERS solid dispersion was taken out and replaced by fresh release medium at 1 hr, 1, 2, 3, 5 day, then the concentration of E_2 was assayed by validated HPLC with the same condition as previously described. After in vitro release study, each implant was dissolved in a mixture of absolute ethanol and dichloromethane (1:1; v:v) and the solution was assayed by UV-spectroscopy (Jasco V-530, Japan) at 280 nm for E_2 residual content. Total E_2 content of each implant was calculated by addition of total E_2 released and residual E_2 content in implant after in vitro release study.

4.2.5 Determination of Drug Release Kinetics

Approximately 60% of E_2 released from each implants was fitted with three different release models: the zero-order, the first-order, and the Higuchi model, by linear regression analysis. The coefficient of determination (R^2) obtained from each fit was used as a criterion to choose the best model for drug release phenomena.

4.2.6 Characterization of E_2 Solid State in Solid Dispersions

4.2.6.1 Polarized Light Microscopy (PLM)

An Olympus BX51 polarized light microscope equipped with a Nikon E990 (Japan) digital camera and Image ProPlus software V4.0 (Media Cybernetics) was used. ERS, solid dispersions containing E_2 at 1, 2, 10, 20, 30 % w/w or E_2 crystal powder was brushed onto a glass slide and covered with a cover-slip. E_2 solid state in these samples was observed under polarized light plus purple light generator. The objective and the ocular magnification was 10x, so that the total magnification was equal to 100.

4.2.6.2 X-ray Powder Diffractometry (XRPD)

A Siemens D5000 diffractometer (Stuttgart, Germany) was used. E_2, solid dispersions containing E_2 at concentration range of 1-75 % w/w, and ERS were scanned from 5° to 90° 2θ (sampling interval of 0.02°) using Ni-filtered Cu Kα radiation. Operating voltage and current were 40 kV and 30 mA, respectively.

4.2.6.3 Differential Scanning Calorimetry (DSC)

A DSC TA Q100 with a refrigerated cooling system (TA Instruments, New Castle, DE) and nitrogen as purge gas was used. The calorimeter was calibrated using indium and sapphire for temperature and heat capacity, respectively. E_2 of 3.17 mg was added to standard aluminum pan with cover and scanned using the following heating program: heating up to 182 °C at 10 °C/min; cooling down to 0 °C at 20 °C/min; heating up to 250 °C at 10 °C/min.

4.2.6.4 Thermogravimetric Analysis (TGA)

A TGA/SDTA 851e with a refrigerated cooling system (Mettler Toledo, Switzerland) and nitrogen as purge gas was used. E_2 was added in an open pan and scanned from 0-750 °C at heating rate of 5 °C/min. Weight loss was determined gravimetrically.

4.2.6.5 Modulated Temperature Differential Scanning Calorimetry (MTDSC)

A MTDSC TA Q100 with a refrigerated cooling system (TA Instruments, New Castle, DE) and nitrogen as purge gas was used. Each sample of E_2, solid dispersion containing E_2 at concentration range of 1-90 % w/w, or ERS was added to standard aluminum pans with covers and scanned using two heating programs. Heating program I: heating from 25 to 120 °C at 10 °C/min; cooling down to 25 °C at 20 °C/min, an isothermal period for 5 min at 25 °C, and finally heating to 250 °C at 5 °C/min. Heating program II: heating from 25 to 182 °C at 10 °C/min, cooling down to 25 °C at 20 °C/min, an isothermal period for 5 min at 25 °C, and finally heating to 250°C at 5 °C/min. A modulation amplitude of ±1°C and a period of 60 s were used.

4.3 Results and Discussion

4.3.1 Effect of Weight Percent of E_2 in ERS Solid Dispersion on E_2 Release Profile

E_2 release profiles of implants containing 1 and 2 % w/w E_2 in ERS solid dispersion are shown in Figure 4.1 (a). E_2 was rapidly released from implants containing 1 and 2 % w/w E_2 in ERS solid dispersion. Approximately 60 % of E_2 were released from those implants within 3 days. E_2 release profiles of implants containing 10, 20 and 30 % w/w E_2 in ERS solid dispersion are shown in Figure 3.3. Percent cumulative releases of E_2 from these implants increased linearly with time. Approximately 60 % of E_2 were released from these implants within 5 days. This indicated that higher weight percent of ERS did not extend E_2 released for longer period. Figure 4.1 (b) illustrates E_2 daily release rates obtained from implants containing 1 and 2 % w/w E_2 in ERS solid dispersion. E_2 daily release rates from those implants drastically decreased with time whereas E_2 daily release rates obtained from implants containing 10, 20 and 30 % w/w E_2 in ERS solid dispersion were rather constant during 1-5 days as shown in Figure 3.4.

When approximately 60 % of experimental E_2 released from implants containing solid dispersions at different E_2 to ERS ratios were fitted with the zero-order, the first-order or the Higuchi release models by linear regression analysis, the coefficient of determination (R^2) obtained from each fit is shown in Table 4.1. It is apparent that the zero-order model might not be a suitable model which could be used to describe the E_2 released from implants containing 1 and 2 % w/w E_2 in ERS solid dispersion compared with the first-order and the Higuchi models. The first-order model describes drug release in a way that is proportional to the amount of drug remaining in its interior, in such way that the amount of drug released by unit of time diminishes (Costa and Lobo, 2001). The Higuchi model describes drug release in a way that the fraction of drug released is proportional to the square root of time. Alternatively, the drug release rate is proportional to the reciprocal of the square root of time (Siepmann and Peppas, 2001). Thus, the release rate of controlled release system described by these two models would become time dependent. This corresponded to decrease E_2 daily release rates with time of implants containing 1 and 2 % w/w E_2 in ERS solid dispersion. Furthermore, the Higuchi model describes drug release based on diffusion mechanism. A proportionality between the cumulative amount of drug released and the square root of time is commonly regarded as an indicator for diffusion-controlled drug release (Siepmann and Peppas, 2001). Thus, E_2 release profiles obtained from implants containing 1 and 2 % w/w E_2 in ERS solid dispersion which could be described by the Higuchi model indicated that diffusion process was the dominating mechanism in these systems.

(a)

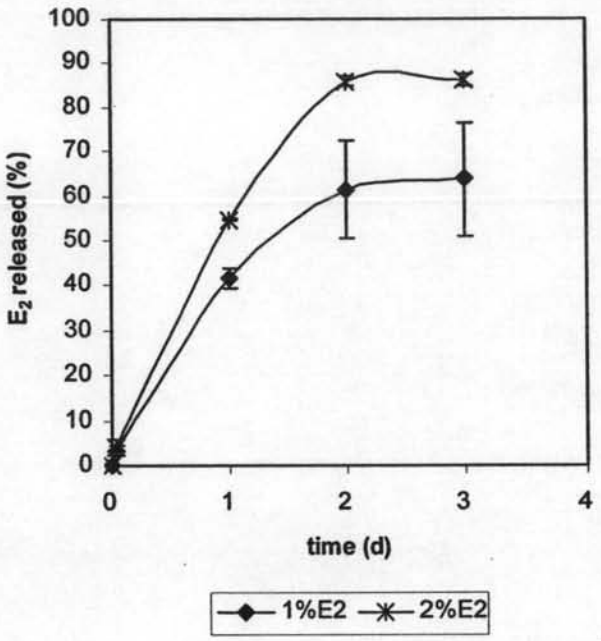

(b)

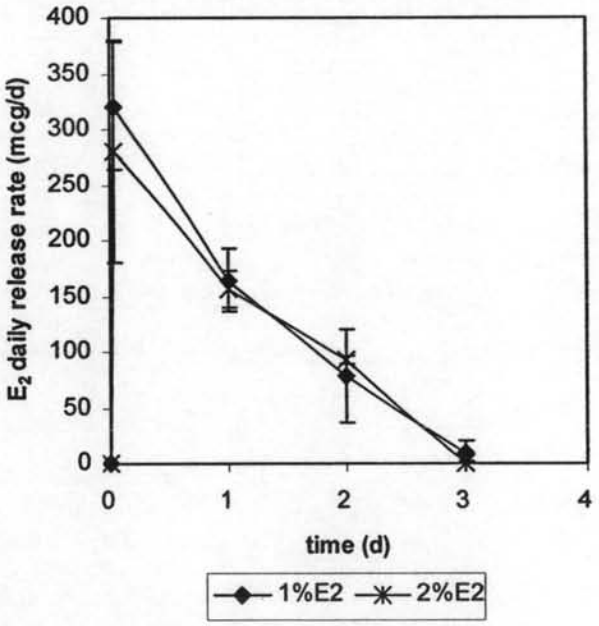

Figure 4.1 E_2 release profiles (a) and E_2 daily release rates (b) from implants containing 1 and 2 % w/w E_2 in ERS solid dispersion

Table 4.1 R^2 obtained from fitting approximate 60 % of E_2 released with the zero-order, the first-order, and the Higuchi models

Weight percent E_2 in implant (n=3)	R^2		
	$Q_t = Q_0 + k_0t$	$Q_t = Q_0 \, x \exp(-k_1t)$	$Q_t = k_Ht^{1/2}$
1%E_2	0.9703	0.9977	0.9933
2%E_2	0.9821	0.9895	0.9897
10%E_2	0.9995	0.9835	0.9368
20%E_2	0.9980	0.9684	0.9320
30%E_2	0.9946	0.9567	0.8978

Q_t, the amount of drug released at time t; Q_0, the initial amount of drug released; k_0, the zero-order release rate constant; k_1, the first-order release rate constant; k_H, the Higuchi dissolution rate constant.

For implants containing 10, 20 and 30 % w/w E_2 in ERS solid dispersion, R^2 obtained from fitting 60 % of experimental E_2 released with the zero-order model were the highest of all release models. The zero-order model describes the system releasing the same amount of drug by unit of time. This release model was in agreement with constant E_2 daily release rates obtained from implants containing 10, 20 and 30 % w/w E_2 in ERS solid dispersion during 1-5 days. This indicated that E_2 daily release rates under this condition would become time independent. Kurnik and Potts (1997) used a combined dissolution- and diffusion-controlled release system for describing the effect of crystal particle size on the release of estradiol from polymer matrices in water. This system explains drug release following two processes. The drug first dissolves in the release medium in the matrix and then diffuses out of the matrix. When the dissolution rate is slower than the diffusion rate of the drug, the former rate markedly influences the drug release and the zero-order release can be obtained (Chandrasekaran and Paul, 1982; Kim, 2000b). This indicated that dissolution rate of E_2 in implants containing 10, 20 and 30 % w/w E_2 in ERS solid dispersion was the dominating mechanism. Furthermore, Chang and Himmelstein (1990) indicated that the zero-order release could not be obtained for system having a high dissolution rate constant of drug. These suggested that dissolution rate of E_2 in implants containing 1 and 2 % w/w E_2 in ERS solid dispersion was higher than that of E_2 in implants containing 10, 20 and 30 % w/w E_2 in ERS solid dispersion. The dissolution rate of E_2 in implants containing 1 and 2 % w/w E_2 in ERS solid dispersion did not offer as the limiting resistance to drug release, so that the zero-order release could not be achieved. On the contrary, the dissolution rate of E_2 in implants containing 10, 20 and 30 % w/w E_2 in ERS solid dispersion performed as the limiting resistance to drug release. Thus, 60 % of E_2 release followed the zero-order kinetic.

4.3.2 Effect of Weight Percent of E_2 in ERS Solid Dispersion on E_2 Solid State

4.3.2.1 E_2 Solid State Characterized by PLM

PLM was used to examine the solid state of E_2 in solid dispersions. An amorphous solid observed under polarized light microscope normally manifests the absence of birefringence because the structure of an amorphous material usually possesses short-range molecular arrangement but lacks long-range translational-orientation symmetry and has regions of different density (Yu, 2001; Sacchetti and Zhu, 2002). Thus, amorphous solid cannot turn plane polarized light and cannot reflect purple light to other wavelengths in range of the spectrum. In any way, the birefringence is always observed in a crystalline material because the crystalline state exhibited regular pattern of molecular arrangements. The molecules in a crystal arranged in a fixed pattern in three dimensions known as a lattice (Gioielli, 2003). Thus, crystalline solid can turn plane polarized light and can reflect purple light to other wavelengths in range of spectrum.

Photomicrographs of ERS, solid dispersion containing 1, 2, 10, 20, 30 % w/w E_2 in ERS and E_2 under polarized light microscope are shown in Figure 4.2. The absence of birefringence was observed in ERS, 1 and 2 % w/w E_2 in ERS solid

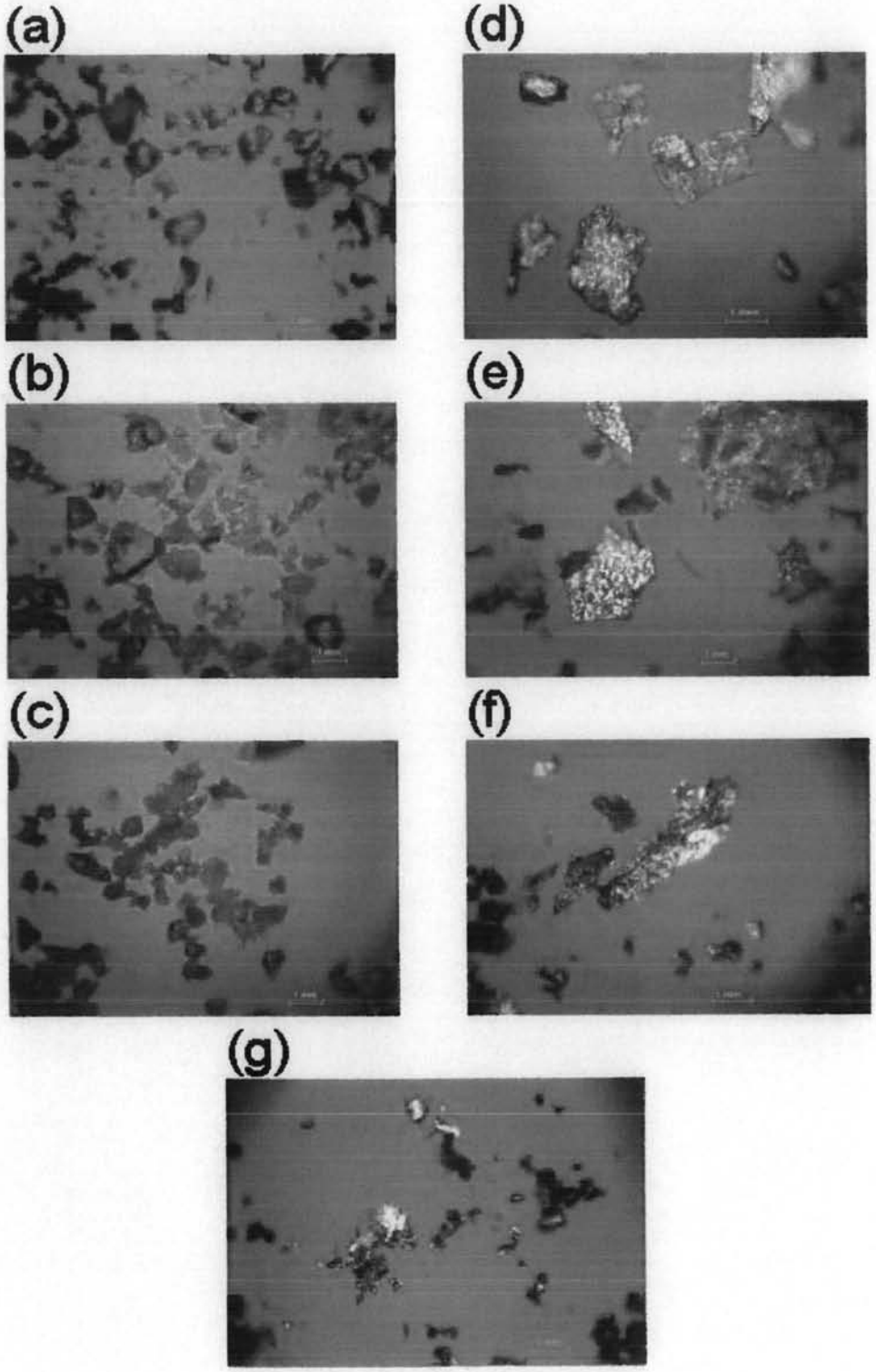

Figure 4.2 Photomicrographs obtained from polarized light microscope: (a) ERS; solid dispersion containing weight percent of E_2 at (b) 1; (c) 2; (d) 10; (e) 20; (f) 30; (g) E_2

dispersion under polarized light microscope as shown in Figure 4.2 (a)-(c). This indicated that E_2 was in an amorphous state in 1 and 2 % w/w E_2 in ERS solid dispersion because these two solid dispersions could not turn plane polarized light and could not reflect purple light to other wavelengths in range of the spectrum. In comparison with 10, 20, and 30 % w/w E_2 in ERS solid dispersions, the birefringence was observed under polarized light microscope as shown in Figure 4.2 (d)-(f). This phenomenon was also observed in E_2 crystal powder as shown in Figure 4.2 (g). These solid dispersions could turn plane polarized light and could reflect purple light to other visible wavelengths as same as E_2 crystal did, so that the solid state of E_2 in these solid dispersions was similar to E_2 crystal, that is, a crystalline state.

4.3.2.2 E_2 Solid State Characterized by XRPD

X-ray powder diffraction patterns of ERS, E_2, and E_2 in ERS solid dispersions at concentration range of 1-75 % w/w are shown in Figure 4.3. X-ray powder diffraction patterns of E_2 exhibited characteristic peaks at a diffraction angle of 2θ, at 13.14, 15.74, 18.26, 22.62, and 26.58° as shown in Figure 4.3 (a). These values and the diffraction pattern were comparable to those reported by Latsch et al. (2003) and Park et al. (2005) characterizing E_2-hemihydrate crystal. These characteristic peaks were also observed in X-ray powder diffraction patterns of E_2 in ERS solid dispersions at concentration range of 10-75 % w/w as shown in Figure 4.3 (b)-(f) but the relative peak intensity and the distinct X-ray pattern decreased in relation to the decrease in weight percent of E_2. However, these characteristic peaks could not be observed in X-ray powder diffraction patterns of 1 and 2 % w/w E_2 in ERS solid dispersion as shown in Figure 4.3 (g)-(h). X-ray powder diffraction patterns of these two solid dispersions did not exhibit a distinct X-ray pattern as same as that of ERS. This is a nature of an amorphous solid. This result indicated an amorphous state of E_2 in 1 and 2 % w/w E_2 in ERS solid dispersion characterized by XRPD. Due to an amorphous nature of ERS, higher weight percent of ERS corresponding to lower weight percent of E_2 in solid dispersion resulted in less crystalline fraction. Thus, the relative peak intensity of those characteristic peaks decreased as fraction of E_2 crystal decreased. However, those characteristic peaks were observed in solid dispersions containing E_2 at 10, 20 and 30 % w/w. E_2 existed in a crystalline state in these concentrations. Therefore, the E_2 solid state in solid dispersion examined by XRPD analysis agreed with that examined by PLM.

4.3.2.3 E_2 Solid State Characterized by Thermal Analysis

4.3.2.3.1 DSC and TGA

DSC curve of E_2 is shown in Figure 4.4. In the first heating run (1), three endothermic peaks were observed. The first two endothermic peaks corresponded to the weight loss around 3.20 % as shown in the thermogravimetrical (TGA) curve of E_2 (Figure 4.5). The third endothermic peak at 179.24 °C was the melting point of E_2. This corresponded with that of E_2-hemihydrate assigned to EA form according to the Variankaval, Jacob, and Dinh (2000) study. The weight loss around 3.20 % indicated that the stoichiometry of E_2 should be $C_{18}H_{24}O_2.\frac{1}{2}H_2O$. The DSC curve during cool down exhibited T_g of E_2 around 84.20 °C corresponding to T_g

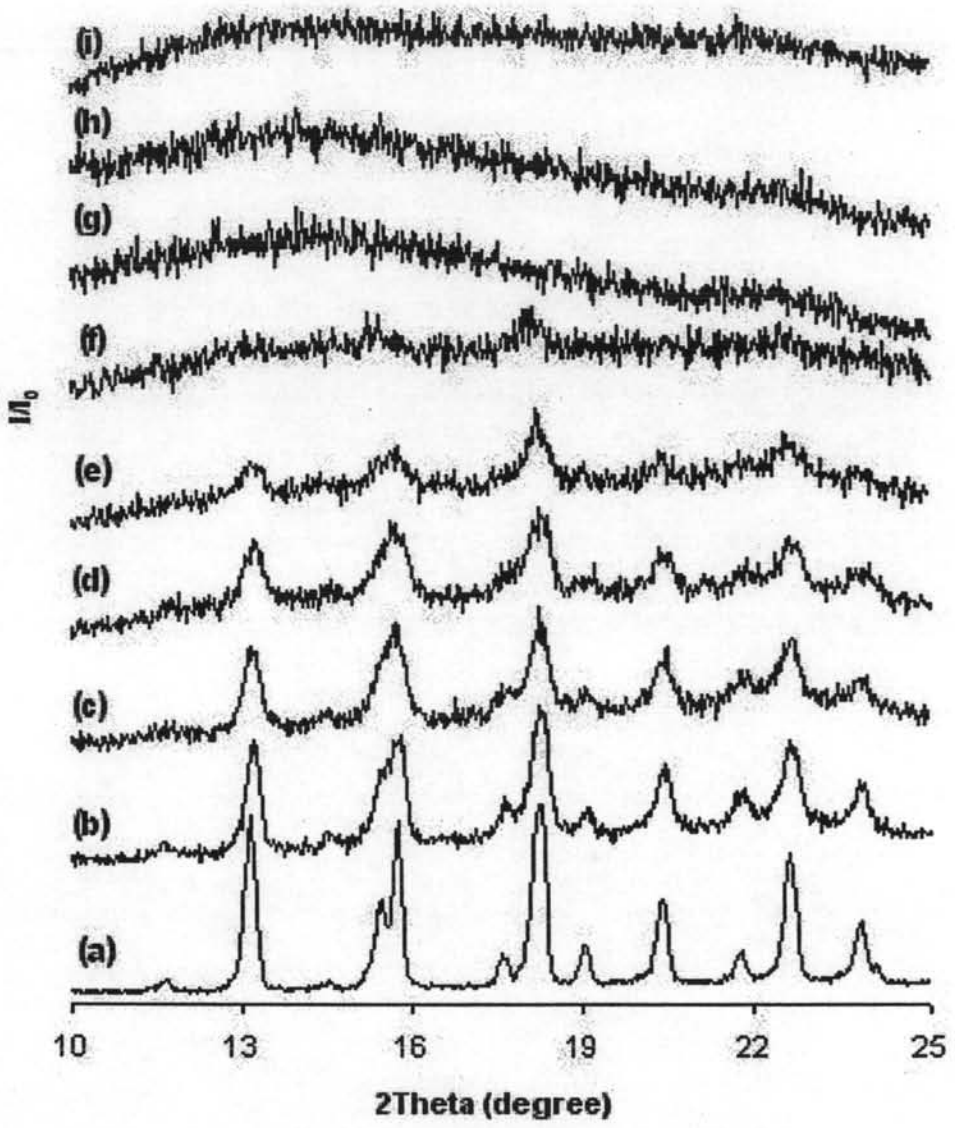

Figure 4.3 X-ray powder diffraction patterns of solid dispersions containing E_2 at different weight percent: (a)E_2; (b) 75 % E_2; (c) 50 % E_2; (d) 30 % E_2; (e) 20 % E_2; (f) 10 % E_2; (g) 2 % E_2; (h) 1 % E_2; (i) ERS

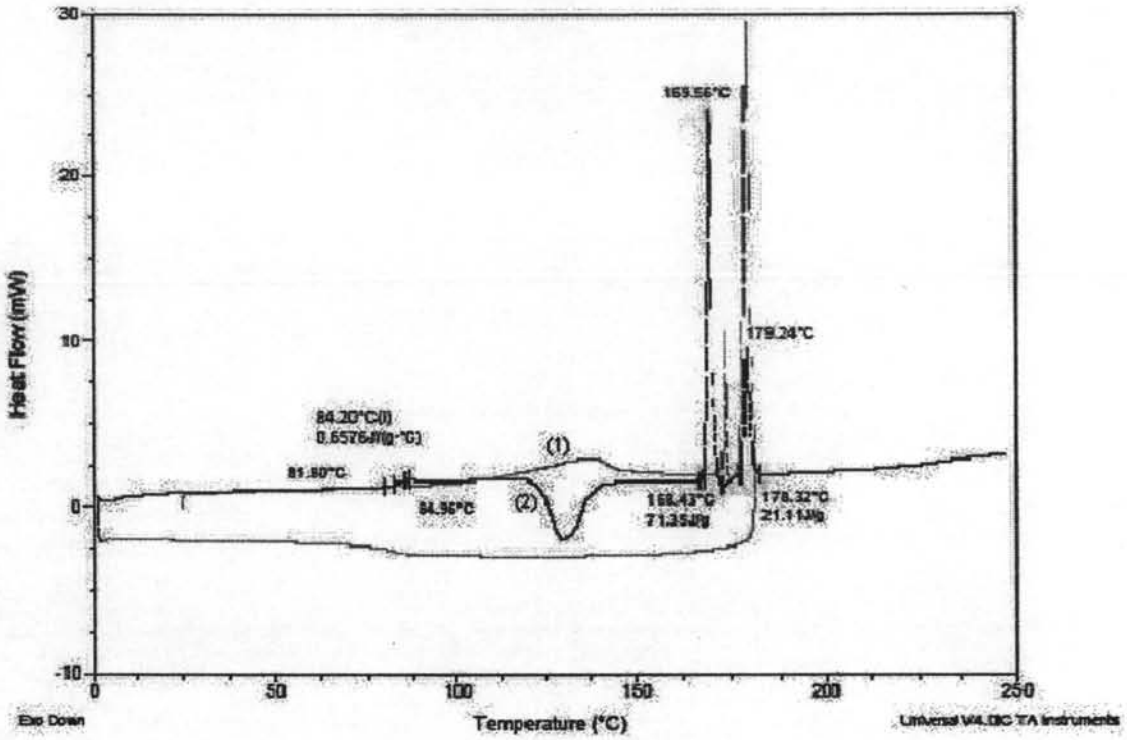

Figure 4.4 DSC curve of E_2 scanned with heating program: (1) heating up to 182 °C at 10 °C/min; cooling down to 0 °C at 20 °C/min; (2) heating up to 250 °C at 10 °C/min

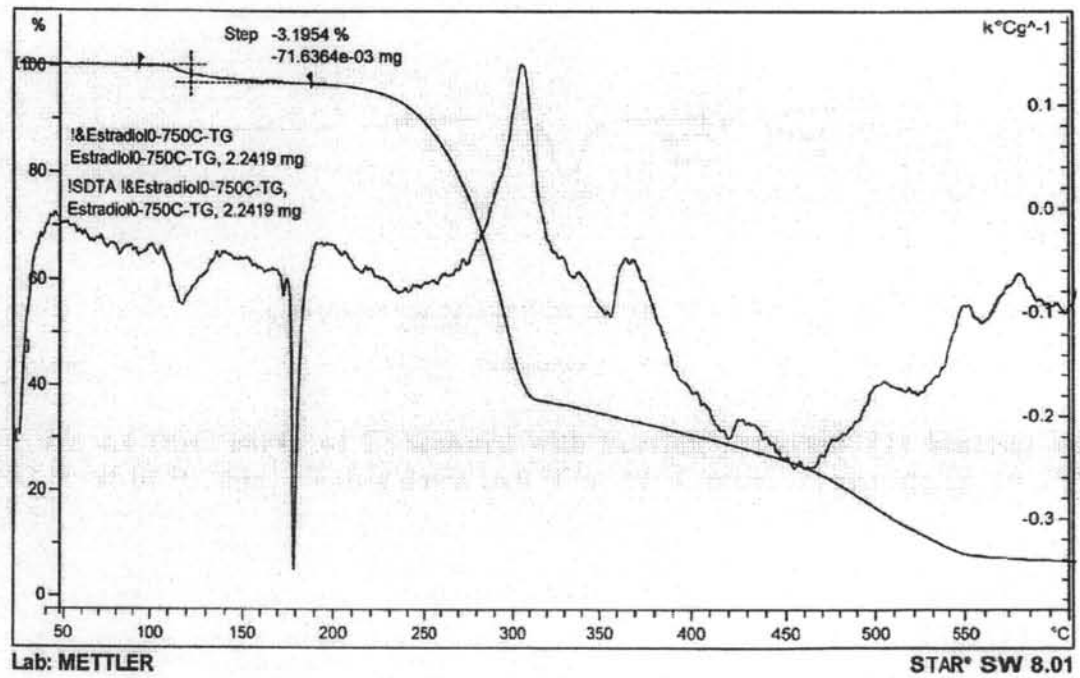

Figure 4.5 TGA curve of E_2

of E_2 observed in the second heating run (2). This indicated that E_2 changed to an amorphous form after heated to 182 °C and then rapidly cooled down because of manifesting T_g from its amorphous nature. In the second heating run, the amorphous form of E_2 in the glassy state was changed to the rubbery state when the temperature was higher than 80 °C. Exothermic peak in the second heating run was observed around 126 °C, followed by two endothermic peaks at 169.56°C and 179.24°C. This result agreed with that obtained by Variankaval et al. (2000) indicating that the first and the second endothermic peaks were assigned to ED form and EC form of E_2, respectively.

The result suggested that T_g of E_2 could be observed when E_2 existed in an amorphous form. In order to differentiate E_2 solid state in solid dispersion in the following experiment, two indicators, i.e. T_g behavior of a blend and melting point of E_2 in solid dispersion, were investigated. In solid dispersion containing amorphous E_2, T_g should lie between those of E_2 and ERS based on the behavior of an amorphous blend in multi-component system (Yu, 2001). In solid dispersion containing crystalline E_2, T_g should belong to T_g of ERS only and the melting point of crystalline E_2 should be observed.

4.3.2.3.2 MTDSC

From MTDSC analysis with heating program I, T_g behavior of solid dispersion containing E_2 at concentration range of 0-90 % w/w examined from reverse heat flows is shown in Figure 4.6 (a). T_g values of E_2 in ERS solid dispersion at concentration range of 1-90 % w/w obtained from MTDSC using heating program I were not different from T_g value of ERS whereas T_g values of those obtained from MTDSC using heating program II increased toward T_g value of amorphous E_2 when weight percent of E_2 increased as shown in Figure 4.6 (b). The resulting T_g of blends obtained from MTDSC using heating program II were affected by T_g of amorphous E_2 and ERS. This is the nature of an amorphous blend as described by the principle of Gordon-Taylor equation (Patterson et al., 2006; Yu, 2001; Fukuoka, Makita, and Yamamura, 1989; Craig et al., 1999). This indicated that E_2 in solid dispersion examined by MTDSC with heating program II existed in an amorphous state.

In DSC curve of E_2, T_g of E_2 was observed during the second heating run. Thus, solid dispersion during the second heating run of heating program II analysis contained amorphous E_2 blended with ERS. In comparison with the resulting T_g of blends obtained from MTDSC using heating program I, T_g behavior deviated from the nature of an amorphous blend. This indicated that E_2 in solid dispersion during analysis with heating program I existed in a crystalline state. Thus, solid dispersion containing E_2 at concentration higher than its solubility in ERS obtained from co-evaporation was composed of crystalline E_2 blended with ERS, which was not described by the principle of Gordon-Taylor equation. This corresponded to the existing of melting point of crystalline E_2 in solid dispersion examined by MTDSC with heating program I as shown in Figure 4.7. Pure crystalline E_2 manifested its melting point at 179.88°C. The melting point of crystalline E_2 decreased when the concentration of ERS in solid dispersion increased. This is the nature of crystalline component blended with an amorphous component

(a)

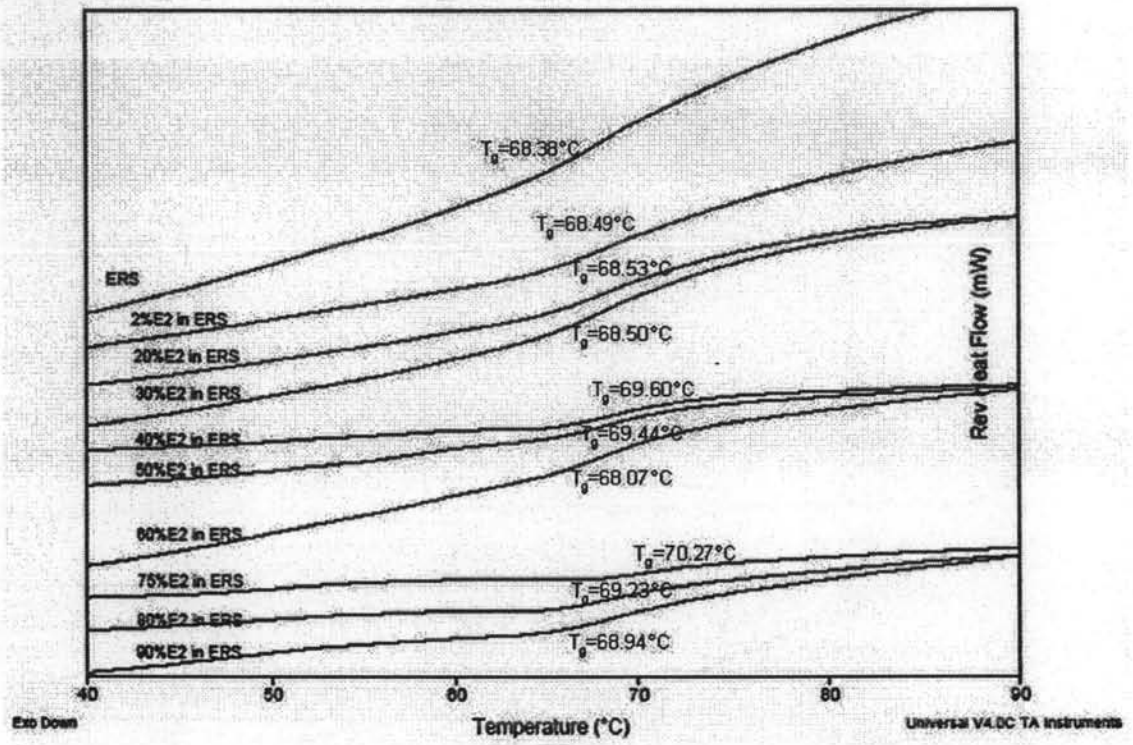

(b)

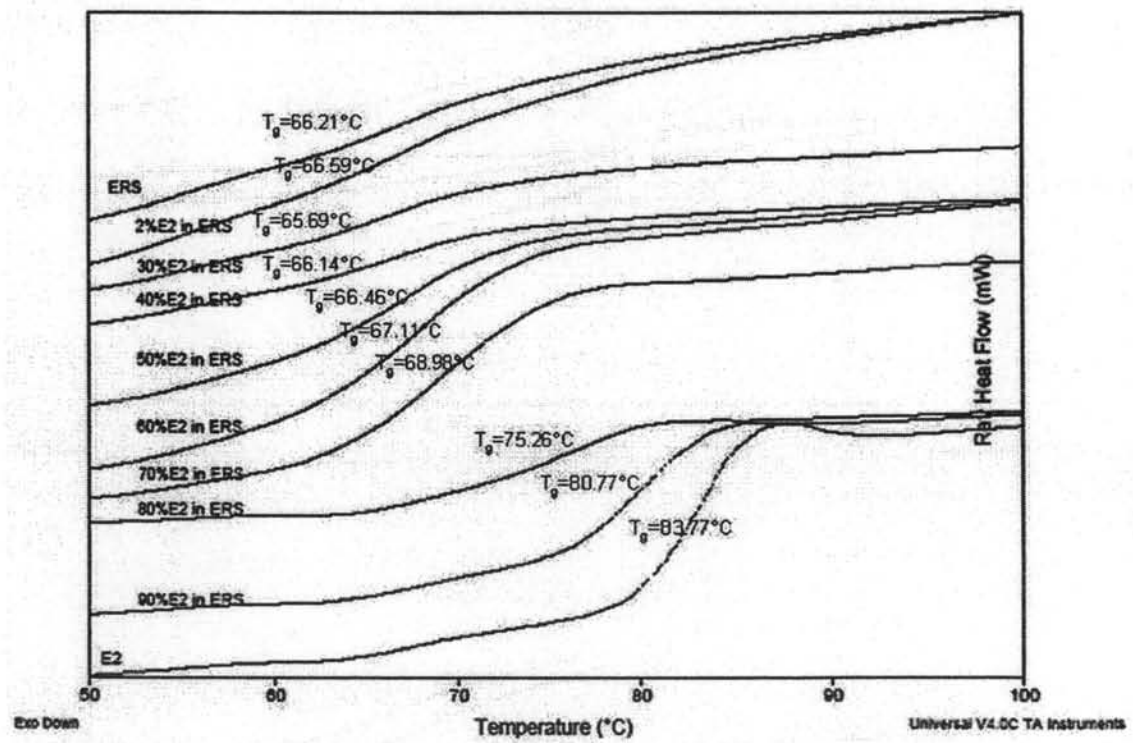

Figure 4.6 T_g behavior of E_2 in ERS solid dispersions at concentration range of 0-100 % w/w obtained from MTDSC: (a) heating program I; (b) heating program II

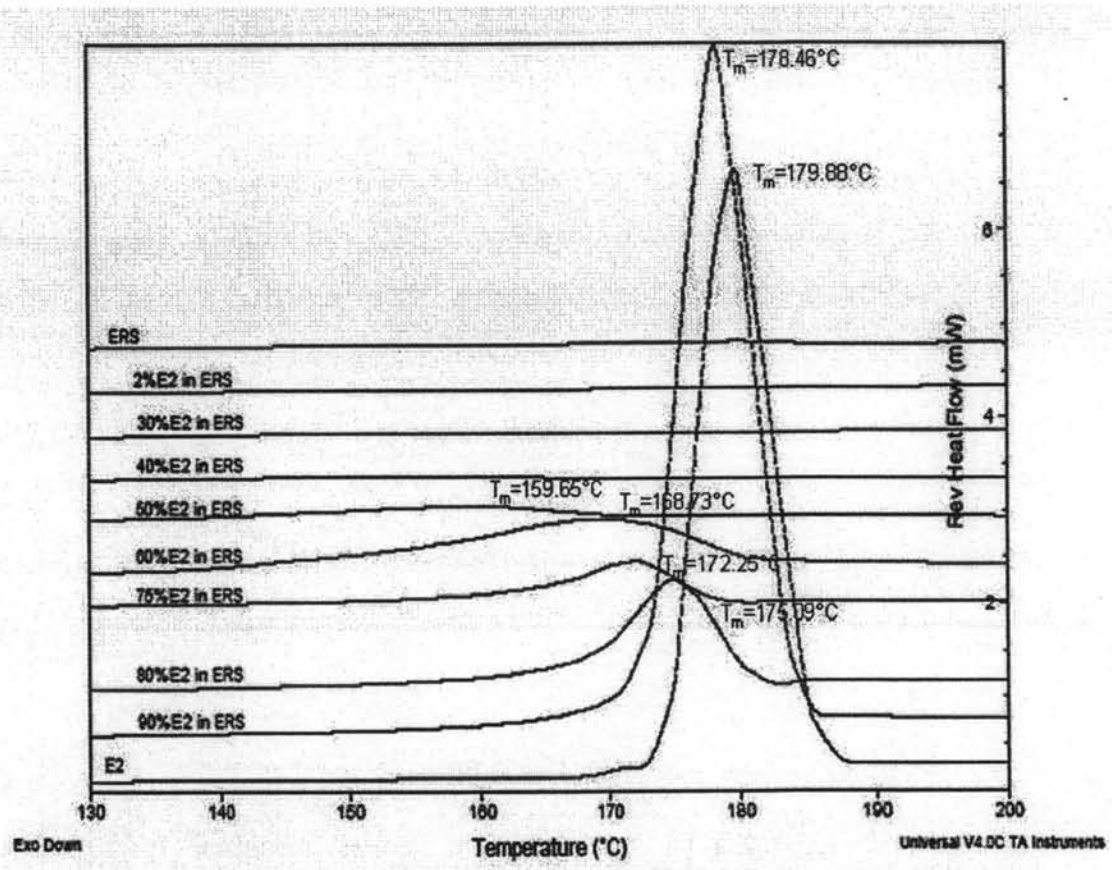

Figure 4.7 The melting point depression of E_2 in ERS solid dispersions at concentration range of 0-100 % w/w obtained from MTDSC scanning with the heating program I

(Tantishaiyakul et al., 1996; Kuo and Chang, 2001; Kuo et al., 2001; Satit Puttipipatkhachorn et al., 2001). The addition of ERS as an amorphous component decreased the chemical potential of crystalline E_2 and led to a reduction of melting point explained by the Flory-Huggins theory (Rostami, 2000; Pimbert et al., 2002).

At lower weight percent of E_2 in solid dispersion, T_g of a blend examined by MTDSC using either heating program I or heating program II were not different from T_g of ERS. This phenomenon could also be explained by the principle of Gordon-Taylor equation. The Gordon-Taylor equation predicts T_g of an amorphous blend based on weight fractions (w) and T_g of its components and allows K to be calculated using amorphous density (ρ) as shown in previously described equation (2.16) and (2.17), respectively (Patterson et al., 2006; Craig et al., 1999; Schneider, 1988).

$$T_g = \frac{w_1 T_{g1} + w_2 T_{g2}}{w_1 + K w_2} \qquad 2.16$$

$$K = \frac{\rho_1 T_{g1}}{\rho_2 T_{g2}} \qquad 2.17$$

Thus, effect of amorphous E_2 properties on the resulting T_g of a blend was trivial. T_g of solid dispersions containing lower weight percent of E_2 were nearly similar to T_g of ERS.

4.4 Conclusions

E_2 existed in an amorphous state in solid dispersion containing 1 and 2 % w/w E_2 in ERS. E_2 dissolution rate did not act as the limiting resistance to drug release from implants containing these solid dispersions. These implants released E_2 in a way that deviated from the zero-order kinetics. In solid dispersion containing 10, 20 and 30 % w/w E_2 in ERS, E_2 existed in a crystalline state. E_2 dissolution rate offered as the limiting resistance to drug release from implants containing these solid dispersions. E_2 released from these implants could be described by the zero-order model.